Periodic and disordered polytypes of SiC: A dynamic model based on local deformations

Gerard L. Vignoles, Roger Naslain

Periodic and disordered polytypes of SiC: A dynamic model based on local deformations

G. L. VIGNOLES
and
R. NASLAIN
Laboratoire des Composites ThermoStructuraux
3,Allée La Boëtie – Université Bordeaux 1
F33600 PESSAC, France
vinhola@lcts.u-bordeaux1.fr

Proceedings of *"High Temperature Ceramic Matrix Composites (HT-CMC2)"*,
R. Naslain, J. Lamon and D. Doumeingts, eds.,
Woodhead Publishing, Abington-Cambridge, UK (1993) ,
pp.249-258.

ABSTRACT

Silicon carbide exists under a great variety of polytypes that can be described by a sequence of orientations of biatomic Si-C layers in a stacking direction. A **dynamical model** is proposed for the formation of polytypes during the layer-by-layer growth of the material that occurs in CVD/CVI. A recurrence law is determined for the sequence of layer deformations ; the orientation sequence is derived from it. The evolution of this law allows one to reproduce qualitatively the whole polytypism of SiC: short- or long-period periodic polytypes, as well as one-dimensionally disordered polytypes. A two-parameter bifurcation diagram has been studied : its fractal structure allows one to visualize various types of "roads to chaos".

INTRODUCTION

Silicon carbide is used, among others, as matrix in ceramic matrix composites (CMC) owing to its high melting point (T_d ~ 2500°C), its stiffness (E ~ 450 GPa), its low density (~ 3.2 g. cm^{-3}) and its excellent behavior in oxiding atmospheres (passive regime). It is deposited chemically from a gaseous precursor (*e. g.* a mixture of CH_3SiCl_3 (MTS) and hydrogen), in the pore network of a porous preform by the so-called chemical vapor infiltration (CVI) process, at a temperature (*i. e.* 900-1100°C) much lower than the decomposition temperature of SiC /1-3/. The nature of silicon carbide in the matrix of SiC-based CMC has been the subject of very few studies /4,5/ and is still an open question.
Silicon carbide is known to display a great variety of crystallographic forms, called polytypes, differing only along a stacking direction of plane, compact, biatomic layers (hereby referred to as bilayers). There are more

than 170 known polytypes exhibiting periodic orientation sequences /6-8/. Some of these structures display very large spatial periods ; others illustrate the phenomenon of one-dimensional disorder /8,9/. This is frequently the case in chemical vapor deposition (CVD) or infiltration (CVI) processes. Direct observation of disordered polytypes in SiC samples synthesized by CVI from a gas mixture of CH_3SiCl_3 (MTS) and hydrogen has been made using high resolution transmission electron microscopy (HRTEM) /4,5/ (fig. 1), showing an abundant random repartition of rotational twins along the growth axis, and Raman spectroscopy /5/,showing a roughly equal intensity for α- and β-SiC phonon peaks.
Although many attempts have been made to explain the occurrence of polytypism, no model accounting simultaneously for the growth of *both* ordered and disordered polytypes has been proposed /10-12/. As the process is such that the chemical system lies **far from thermodynamical equilibrium**, it is not attempted to model polytypism by means of a phase diagram, but rather to build a **dynamical model**. It will be shown how disordered polytypes can appear from deterministic growth mechanisms yielding also all the known polytypes.

1. STRUCTURE DESCRIPTION

Silicon carbide polytypes may be described as different stacking sequences of Si-C bilayers along a $<111>_\beta$ or the $[0001]_\alpha$ direction of the corresponding cubic or hexagonal structures, which are also the only growth directions of interest to control polytypism /6,7,13/. Each bilayer displays a hexagonal arrangement perpendicular to the growth direction /14/. A schematic representation is shown in fig. 2. Every new layer has a choice in orientation as its settles itself up on the former one : it can be deduced from the former layer either by a simple translation, or by a translation plus a 180° rotation. These two options are respectively described by the letters **k** and **h** in Jagodzinski's "**h-k**" notation /15/. The choice leads to two unequivalent atomic environments : when the orientation of the new layer is **h**, its upper atoms are in eclipsed conformation with respect to the lower atoms of the former layer, while they are staggered in **k** orientation /16/. Any polytype can be described by an orientation sequence U_n, n being the integer layer index. U_n is a boolean sequence since it has only two possible values (**h** and **k**). As an example, the 15R polytype, whose Zhdanov notation /17/ is $(23)_3$, will be denoted $(\mathbf{hkhkk})_3$.

2. LOCAL DEFORMATIONS

A detailed study of the structures of various non-cubic polytypes shows that every cristallographic site displays a slight deformation of its coordination tetrahedron, due to atomic interactions. This feature has been evidenced for SiC by different methods. Careful X-ray analyses of 2H-SiC /18/ and 6H-SiC /19/ have allowed previous authors to estimate non-ideal bond lengths and angles. ^{29}Si and ^{13}C NMR studies /20/ reported the existence of 4 different kinds of sites in usual polytypes (3C,2H,4H,6H and 15R) ;

they have been related to the orientation of their layer and of the neighboring one /20,21/. *Ab initio* pseudopotential total-energy calculations on relaxation effects in the bulk structure of 5 simple polytypes /22/ have also been made : they are in reasonable agreement with the X-ray data.
The deformations are elongations of the coordination tetrahedra along the growth axis, *i. e.*, the bond lengths parallel to this axis, which are inter-bilayer bond lengths (hereafter denoted L_n), are longer than the other ones, located inside the bilayers (denoted l_n). The relative difference between them, $\delta_n = (L_n - l_n)/l_n$, is less than 1%. The bond angles do not vary significantly /16,22/. The deformations are variable according to the sites, a feature which leads to suppose that they play an important role in the local stabilization of a given orientation for every new atomic bilayer. If account is not taken of dangling bond rearrangements at the surface, there are only three characteristic geometrical variables at each layer : L_n, l_n, and the angle A_n. However, the first two will be retained since A_n does not vary significantly.
The relation between bond lengths and orientations is sketched in fig. 3, where the lengths for each bilayer, as calculated by Cheng et al. /22/, are represented as a point in the (L_n, l_n) space. The data can be clearly divided into two groups : one of low deformation and of orientation **k**, and one of higher deformation and of orientation **h**. A direct relation between bond distortions and orientations thus appears. Moreover, as the points are roughly aligned along the dotted line, it is possible to restrict oneself to only one variable in order to describe the deformations, for example δ_n ,as defined above, which varies along this line.
Fig. 4 shows the repartition of the different bilayers on a δ_n axis, associated to their orientation U_n. The distinction between the **h** and **k** groups is clear. Going further, they can be split further into four groups, according to the nature of the orientation U_{n+1} of the following layer. These groups fit exactly the NMR shift groups as defined in /20,21/. A further splitting on the criterion of U_{n+2} is possible. The ordering of the arising $U_nU_{n+1}U_{n+2}$ sequences is strikingly regular : if **k** is replaced by 0 and **h** by 1, then they follow the ordering of binary numbers : 000 < 001 < 010 < ....

3. THE ITERATIVE MODEL

The deformations δ_n, as well as the orientations, can be considered as forming a sequence. The description of this real sequence is achieved through the determination of the recurrence law, *i.e.* the function f so that $\delta_{n+1} = f(\delta_n)$. To perform this, one has simply to plot δ_{n+1} as a function of δ_n. Fig. 5 exhibits such a plot, as built using the computation results of Cheng *et al.* /22/. The fitted curves represent portions of the recurrence law f, also called first return map. f appears to be a once discontinuous function increasing on both sides of the discontinuity δ^*, that is, a "sawtooth map" /23,24/. The presence of the discontinuity is related to the change of the layer n from **h** to **k**, and is consistent with the fact that the orientation choice is not based on the δ_n, but on an energetic cri-

terion. Since $\delta_n < \delta^*$ implies $U_n = \mathbf{k}$ and $U_n = \mathbf{h}$ for the converse case, the orientation sequence is directly deduced from the deformation sequence.

4.DYNAMICAL BEHAVIOR

In order to determine the possible dynamical behaviors of the model, an example of a family of maps similar to f, and of simpler analytic formulation, has been studied. This family is generated by varying two parameters λ_1 and λ_2 designed to tune the height of the two continuous parts of f:

$$f_{\lambda_1,\lambda_2}(x) = \begin{cases} 4\lambda_1 x(1-x) & \text{if } x \le 1/2 \\ 1-[4\lambda_2 x(1-x)] & \text{if } x > 1/2 \end{cases}$$

By variation of λ_1 and λ_2 and characterization of the permanent behaviour associated to every couple of parameters, a bifurcation diagram has been computed. By attributing a distinct color to each period between 1 and 256, one obtains the image in fig. 6. This picture has a fractal, *i. e.* self-similar appearance. The domains of dynamical stability of periodic behaviors are fish-like shaped regions obeying to two disposition rules ("fish reproduction rules") :

- Rule R1 : Between the "bodies" of two fishes of periodic sequences $(A_1A_2...A_n)$ and $(B_1B_2...B_m)$ lies a fish of sequence $(A_1A_2...A_nB_1B_2...B_m)$.
- Rule R2 : Between the "tails" of two fishes of sequences $(A_1A_2...A_n)$ and $(B_1B_2...B_m)$ lies a fish of sequence $A_1A_2...\overline{A_n}B_1B_2...\overline{B_m}$, where $\overline{A_n}$ stands for **h** if $A_n = \mathbf{k}$ and reciprocally.

The nature of these laws (and consequently the structure of the diagram) has been demonstrated using the symbolic dynamics derived from the model, *i. e.* the dynamics of orientation sequences rather than the deformation sequences /24,25/. The basic feature lies in the above mentioned equivalence between the ordering of δ_n and of the $U_nU_{n+1}...$ sequences.

A consequence of rules R1 and R2 is that *any* imaginable orientation sequence, either periodic or chaotic, has a corresponding "fish" in the diagram of fig. 6. In particular, all known polytypes of length inferior to 50 have been attributed : they seem to lie in a restricted domain of the diagram, whose contour has been sketched.

The points corresponding to chaotic behavior in fig. 6 form a surface of fractal contour, whose noninteger dimension is roughly 1.6 : this means that chaos is a frequent possibility for the family of maps f_{λ_1,λ_2}. The symbolic approach allows to evidence the presence and the fractal structure of a frontier for topological chaos.

CONCLUSION

The above model, though minimal and very approximative, reproduces the richness of SiC polytypism. Its specificity is the ability to account for the formation of polytypes during SiC growth by CVD/CVI. The *same* physical bases (local interactions between bilayers) are used to describe the apparition of ordered (periodic) polytypes as well as disordered ones. It is possible to locate inside fig. 6 the disordered polytypic se-

quences present in SiC formed by CVI investigated by HRTEM /4,5/ - at least a finite sampling of them - with the help of the algebra of symbolic sequences derived from the iterative model.

ACKNOWLEDGEMENTS

The authors wish to thank SEP and CNRS for financial support and S. Schamm (CEMES-LOE, Toulouse) for providing HRTEM photos of SiC crystals and matrix, and helpful discussions.

REFERENCES

1. E. Fitzer, D. Hegen & H. Strohmeier, "Possibility of Gas Phase Impregnation with Silicon Carbide", Rev. Int. Hautes Temp. Réfract. 17 (1980) 23.
2. R. Naslain & F. Langlais, "CVD Processing of Ceramic-Ceramic Composite Materials", in "Tailoring Multiphase and Composite Ceramics", R. E. Tressler *et al.* eds, Mat. Sci. Res. 20 (1986) 145.
3. D. P. Stinton, T. M. Besmann & R. A. Lowden, "Advanced ceramics by chemical vapor deposition techniques", Amer. Ceram. Soc. Bull., 67(1988) 350.
4. S. Schamm, A. Mazel, D. Dorignac & J. Sévely, "Observation en microscopie électronique à haute résolution du polytypisme du SiC dans la matrice d'un composite SiC/SiC", in "Matériaux Composites pour Applications à Hautes Températures", AMAC/CODEMAC Bordeaux 1990, R. Naslain, J. Lamalle & J. L. Zulian eds (1990) 207.
5. D. P. Stinton, D. M. Hembree Jr., K. L. More, B. W. Sheldon & T. M. Besmann, "Characterization of ceramic matrix composites fabricated by chemical vapor infiltration", in "Chemical vapor deposition of refractory metals and ceramics", eds. T. M. Besmann & B. M. Gallois, Material Research Society Symposium Proceedings, 168 (1990)273.
6. A. R. Verma & P. Krishna, "Polymorphism and Polytypism in Crystals", Wiley, New York. (1966).
7. P. Krishna, "Crystal Growth and Characterization of Polytype Structure", Pergamon Press, New York. (1983).
8. G. R. Fisher & P. Barnes,"Towards a Unified View of Silicon Carbide Polytypism", Philos. Mag. B 61 (1990) 217-236.
9. S. Shinozaki & K. R. Kinsmann, "Aspects of 'One-Dimensional Disorder' in Silicon Carbide", Acta Met. 26 (1978) 769.
10. D. Pandey & P. Krishna, in ref. /2/, 213.
11. G. D. Price & J. Yeomans, "The application of the ANNNI model to polytypic behaviour", Acta Cryst. B40 (1984) 448-454.
12. C. Cheng, V. Heine & I. L. Jones, "Silicon carbide polytypes as equilibrium structures", J. Phys. C : Condens. Matter 2 (1990) 5097-5113.
13. A. R. Verma, "Crystal Growth and Dislocations", Butterworths, London. (1953).
14. W. F. Knippenberg, "Growth Phenomena in Silicon Carbide", Philips Res. Rept. 18 (1963) 161-274.

15. H. Jagodzinski, "One-Dimensional Disorder in Crystals and its Influence on X-Ray Diffraction. Part I", Acta Cryst. 2 (1949) 201-207.
16. W. Weltner Jr., "On Polytypism and Internal Rotation", J. Chem. Phys. 51 (1969) 2469-2483.
17. G. S. Zhdanov, "Le symbole numérique des empilements compacts de sphères et son application dans la théorie des empilements compacts", Compt. Rend. Acad. Sci. URSS 48 (1945) 43.
18. H. Schultz & K. H. Thiemann, "Structure Parameters ans Polarity of the Wurzite Type Compounds SiC-2H and ZnO", Solid State Comm. 32 (1979) 783-785.
19. A. H. Gomes de Mesquita, "Refinement of the Crystal Structure of SiC Type 6H", Acta Cryst. 23 (1967) 610.
20. J. R. Guth & W. T. Petuskey, "Silicon-29 Magic Angle Sample Spinning Nuclear Magnetic Resonance Characterization of SiC Polytypes",J. Phys. Chem. 91 (1987) 5361-5364.
D. C. Apperley, R. K. Harris, G. L. Marshall & D. P. Thompson, "Nuclear Magnetic Resonance Studies of Silicon Carbide Polytypes", J. Am. Ceram. Soc. 74 (1991) 777-782.
21. M. O'Keeffe, "Topological and Geometrical Characterization of Sites in Silicon Carbide Polytypes", Chem. Mater. 3 (1991) 332-335.
22. C. Cheng, V. Heine & R. J. Needs, "Atomic Relaxation in Silicon Carbide Polytypes", J. Phys. C : Condens. Matter 2 (1990) 5115-5134.
23. G. L. Vignoles, "Atomic Relaxation and Dynamical Generation of Ordered and Disordered Chemical Vapour Infiltration (CVI) SiC Polytypes",J. Crystal Growth 118 (1992 430-438.
24. G. L. Vignoles, "Un modèle dynamique simple pour la croissance de polytypes du SiC en CVD/CVI", Ph D. Thesis, Un. Bordeaux I, n° 892 (1993).
25. P. Collet & J.-P. Eckmann, "Iterated Maps on the Interval as Dynamical Systems", Progress in Physics 1, A. Jaffe & D. Ruelle eds., Birkhäuser, Basel-Boston-Stuttgart. (1980).
26. G. L. Vignoles, "Iterations of the sawtooth map as a dynamical model for CVD/CVI SiC polytype growth", submitted to Intl. J. of Bifurcations and Chaos (1993).

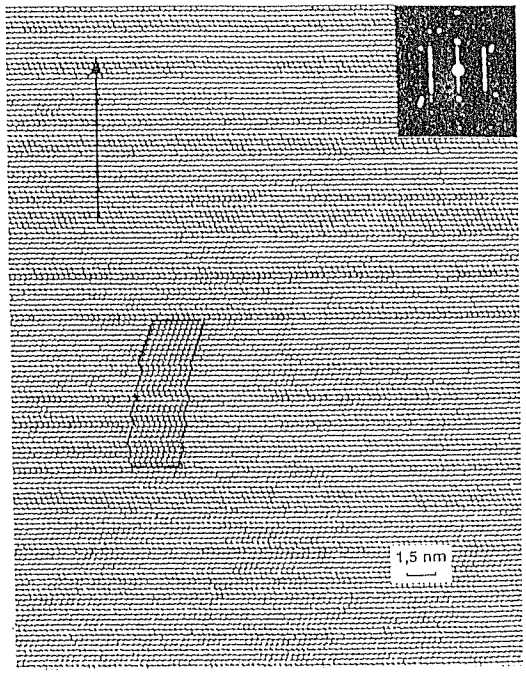

Fig. 1 : HRTEM photograph of a disordered SiC polytype observed along a $<11\bar{2}0>_\alpha$ direction. In the upper right corner, diffraction diagram showing disorder. In the middle left, superposition of a computed image. Image from /4/.

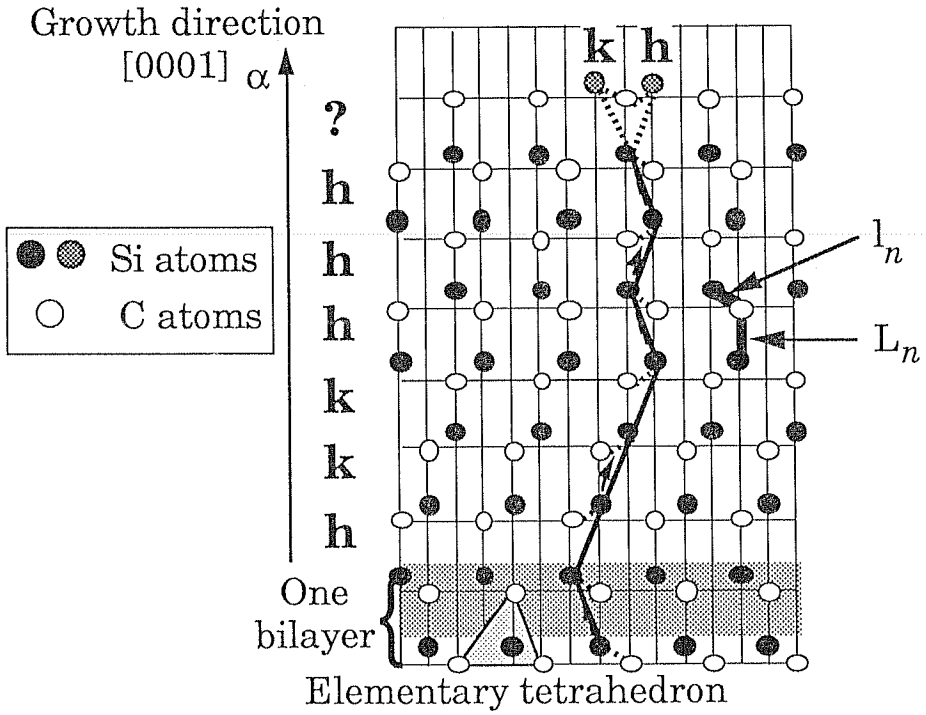

Fig. 2 : Schematic description of a disordered SiC polytype observed along a $<11\bar{2}0>_\alpha$ direction.

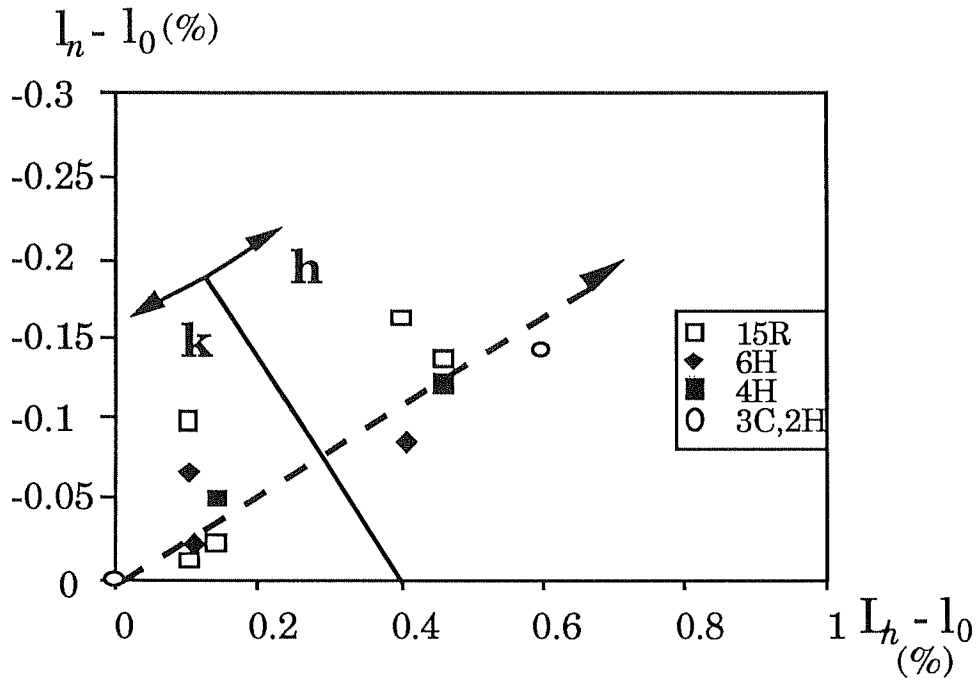

Fig. 3 : Representation of the layers of simple polytypes as points in the (L_n,l_n) space. The values are from /20/, and are given as differences with the ideal bond length l_0 (= L_0).

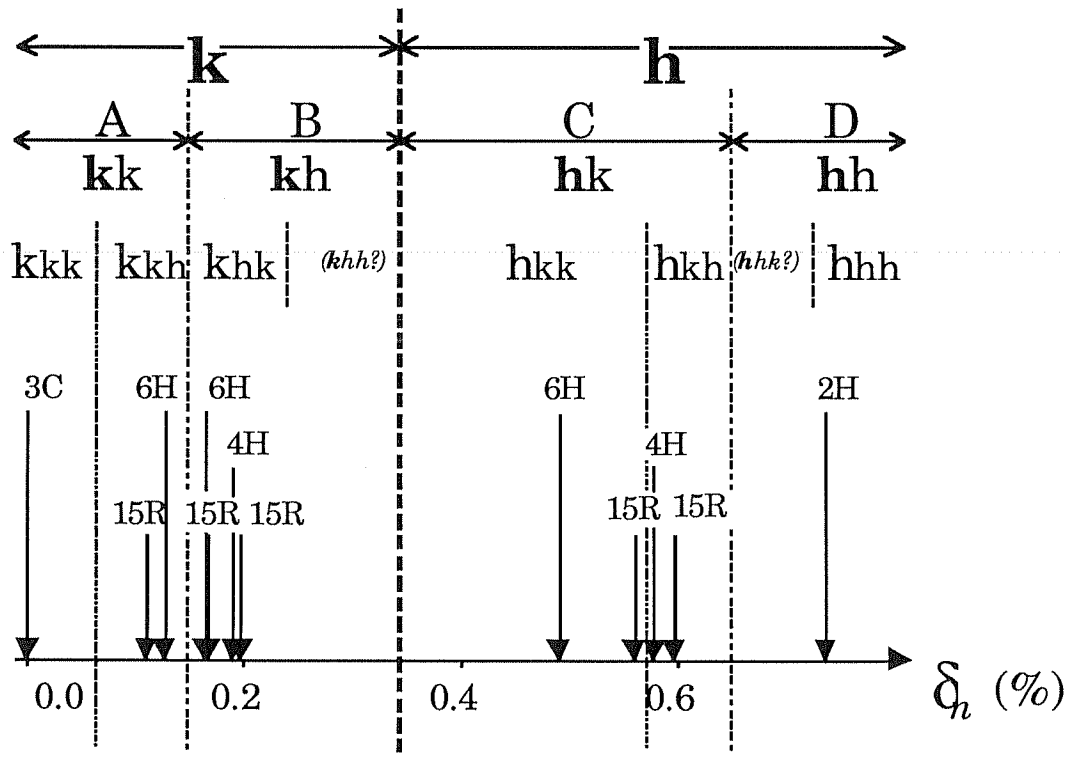

Fig. 4 : Correspondence between deformations δ_n, orientation sequences in terms of **h** and **k** symbols and NMR shift groups (A, B, C and D).

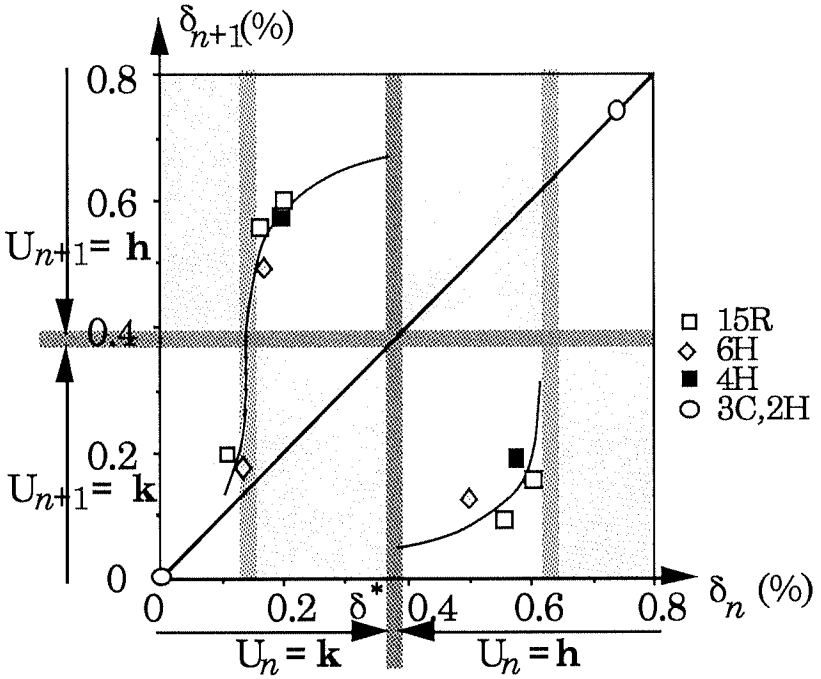

Fig. 5 : First return map of the deformations. The full line is a guess of the recurrence function f.

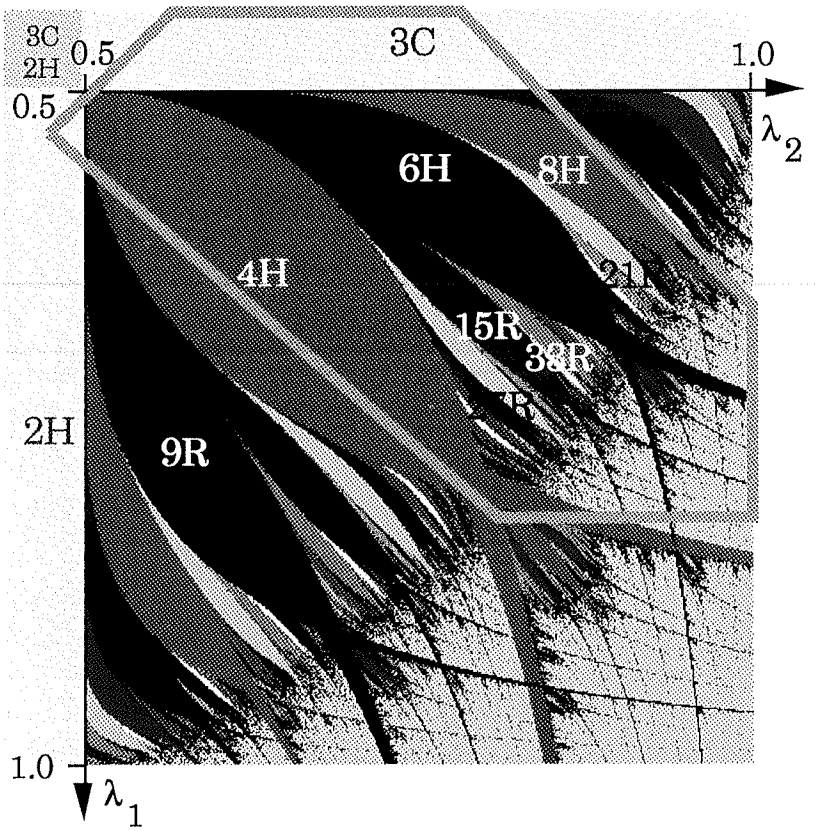

Fig. 6 : 2-parameter bifurcation diagram of the sawtooth map. The skeched contour "contains" all known polytypes of length ≤ 50.

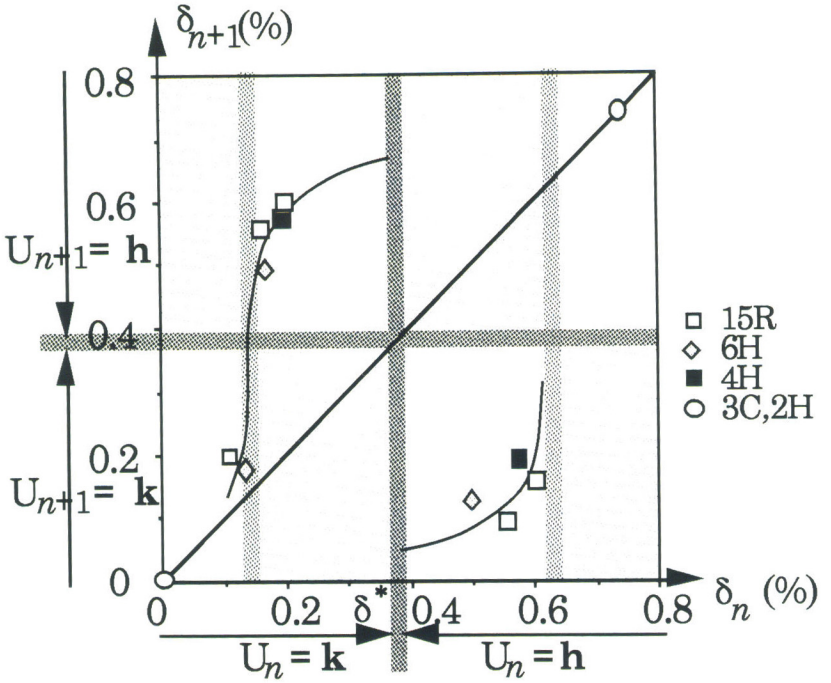

Fig. 5 : First return map of the deformations. The full line is a guess of the recurrence function f.

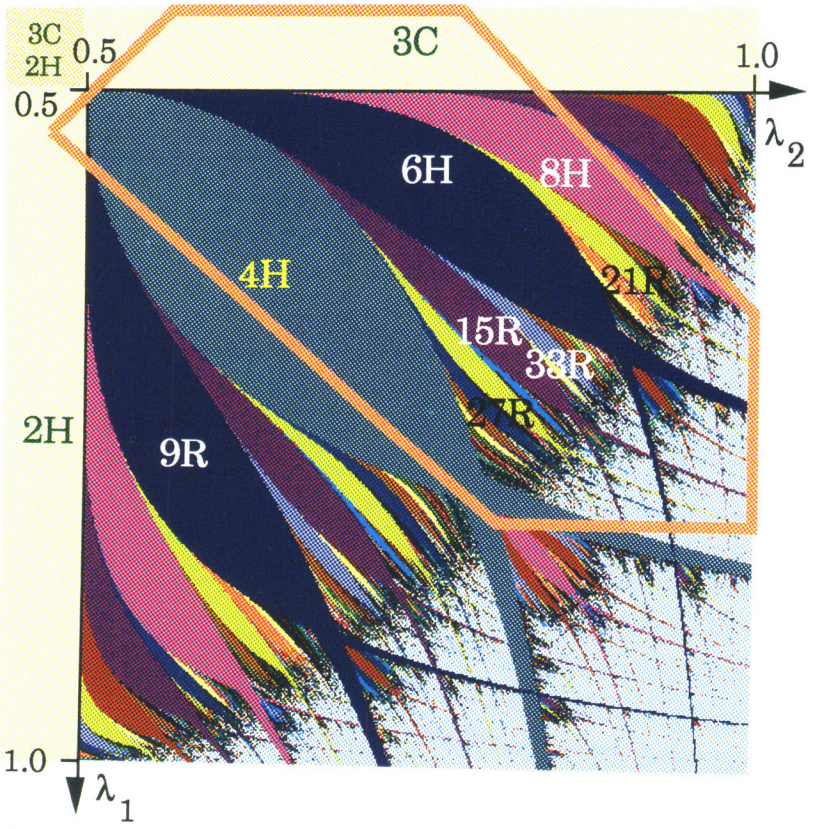

Fig. 6 : 2-parameter bifurcation diagram of the sawtooth map. The skeched contour "contains" all known polytypes of length ≤ 50.